Petrographic examination of concrete from 20th century bridges and identification of reactive components

Š. Lukschová, R. Přikryl and Z. Pertold
Institute of Geochemistry, Mineralogy and Mineral Resources, Faculty of Science, Charles University in Prague, Prague, Czech Republic

ABSTRACT: Eight concrete bridges constructed during the 20th century and affected by alkali-silica reaction (ASR) have been examined macroscopically. Samples taken away were examined by conventional optical microscopy of thin sections, petrographic image analysis and SEM/EDS analysis. All samples show presence of alkali-silica gels which amount ranges from 0.1 to 0.8 vol. %. The presence of gels is controlled by bridge construction data and by volume of specific type of coarse-grained aggregate that was identified as quartzite. Other phases (rock fragments coming from granitoids, volcanic rocks and monomineral clasts like quartz and feldspars) do not show any or very little contribution to the formation of alkali-silica gels.

1 BACKGROUND OF THE ASR DAMAGE OF CONCRETE

Open air cracks and white coatings are the signs of alkali-silica reaction (ASR) macroscopically observed in the concrete surface. In concrete, aggregates containing reactive SiO_2 react with the alkalis sodium and potassium and form amorphous alkali-silica gels. Alkali-silica gel is formed especially in the aggregate or at its margins. It absorbs water molecules, enlarges its volume and exerts pressure. The internal pressure may exceed consistency limits of concrete, which causes mechanical failures (e.g. Hobbs 1998, St John et al. 1998).

The ASR occurs only in the case if three principal factors act mutually: (I) sufficient amount of alkalis, (II) presence of reactive forms of silica in aggregate, and (III) sufficient moisture. The alkalis can be derived from cement, from aggregate and/or from an external source. The critical point is, however, presence of aggregate containing disordered (poorly crystalline) forms of silica like opal, cristobalite or tridymite in e.g. sedimentary or volcanic rocks, or highly strained quartz in some types of metamorphic rocks.

The damage ratio in concrete is determined in extensive body of the literature according to the visual observation carried out “in situ”. More advanced methods use digital image analyses that enables the quantitative analysis of cracking in concrete (Rivard and Ballivy 2005, Rivard et al. 2000). From laboratory techniques different approaches including petrographic study, chemical tests, and dilatometrical evaluation are used to evaluate the ASR potential of aggregates.

1.1 Recent developments in petrographic techniques for the study of alkali-silica reaction

The use of analytical techniques like scanning electron microscopy with energy dispersive spectroscopy (SEM/EDS) and/or X-ray diffraction (XRD) together with standard petrographic examination enhances identification of reactive components (e.g. Peterson et al. 2006). The identification of reactive forms of silica is, however, very difficult task as these cannot be easily separated by optical microscopy from other forms (e.g. St John et al. 1998). This was one of the reasons for the introduction of dilatometrical testing to evaluate the reactivity of aggregates.

The petrographic examination can also facilitate determination of mechanisms of concrete damage even in cases where ASR is accompanied by other processes like frost weathering (Koskiahde 2004). In some cases, the detailed petrographic examination helped detection of the right mechanism of concrete damage – i.e. sulphate attack and formation of ettringite instead of originally proposed mechanism of ASR (Sahu and Thaulow 2004).

1.2 Aims of the study

This study presents part of the project focused on the experimental evaluation of the petrographic factors enhancing ASR in concrete structures.

Aims of this study were to correlate two methods, macroscopical observation "in situ" and petrographical identification of the ASR using optical microscopy and SEM/EEDS, to identify the aggregates causing the ASR and finally to find weather the year of the bridge construction correlate with the extension of ASR.

Eight different bridges were selected that exhibited the following characteristics: 1) the extensive signs of ASR were firstly observed in 1990s, 2) the repairing works were realized in 1995, 3) protective coatings were used, 4) in 2005 the control sampling from the most damaged parts followed in order to evaluate the quality of repair and to examine the remnants of previous ASR, 5) the signs of ASR were repeatedly macroscopically observed. The damages macroscopically observed in concrete are shown in Figure 1. Cracking and spalling were considered as pre-indicators of ASR. The total amount of alkali-silica gels was accepted as reference value of ASR in concrete.

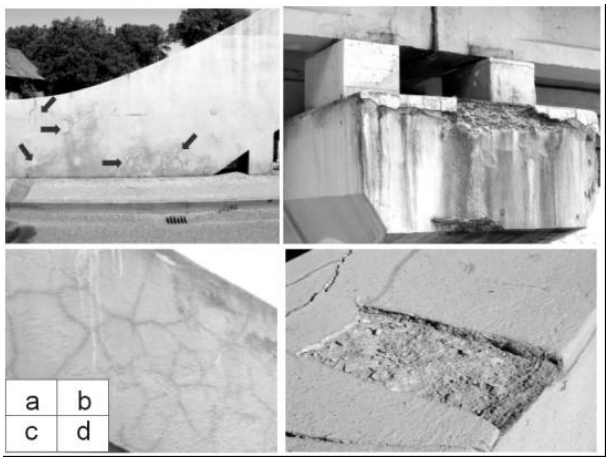

Figure 1: In situ observation of ASR. a) cracks through the face-side (indicated by black arrows), b) front of the pillar damaged by concrete spalling, c) detailed view of the net of cracks, d) detailed view of the spandrel panel over the pillar

2 SAMPLES

2.1 Sites of sampling

The concrete samples were taken from eight concrete bridges located in various places in the Czech Republic. The road bridges were constructed in 1924-1982 period and have been considered as "safe" from the ASR point of view for several years or decades. During inspection in 1990s, the extensive signs of ASR have been, however, located on these structures and repair followed in late 1990s. About five years after the repair (in 2005), the control sampling in the most damaged parts followed in order to evaluate the quality of repair and to examine the remnants of previous ASR. The visual examination of damage ratio was carried out macroscopically "in situ" (according to ČSN 736221) by Pontex Ltd. All bridges show functionless protective coatings and large surface parts damaged by cracks. More detailed descriptions of identified

damages are mentioned in Table 1.

2.2 Sampling and preparation of thin sections

The sampling consisted of diamond-core drilling carried out by Pontex Ltd. The cores show 80 and/or 100 mm in diameter depending on the location of the drill and length from 300 to 400 mm. At each site 1-2 drill cores were taken. The size of the cores allowed preparation of several thin sections in order to overcome the heterogeneity of the material. The remnants were stored for other analyses. Details on sampled bridges and sampling points are given in Table 1.

Table 1 : Summary of studied samples. S.n. – sample n., f.f. – floor framing, * - data accepted from Klier (2005)

s.n.	bridge location	data-tion	damages(*)	sampling point
14-070	Trutnov	1977	in-leak into construction joints, deep concrete degradation, ASR cracks in f.f.	right front of pillar no. 8
14-071	Trutnov	1975	in-leak in construction joints, ASR cracks in f.f.	pillar no. 3
180-010	Dolany	1934	cracks in f.f., moulding surface, spandrel panel surface and in road-fence	spandrel panel over pillar
232-007	Liblín	1929	cracks in f.f., in road surface and in spandrel panel surface	spandrel panel over pillar
272-006	Lysá nad Labem	1973	out of drainage, in-leak, corrosion and ASR cracks in landing fronts	landing front near abutment no. 2
610-018	Stará Boleslav	1982	in-leak into construction joints, corrosion and deep open cracks in f.f. surface	left front of pillar no. 8
610-019	Tuřice	1924	cracks in f.f. surface, corrosion	f.f. arc over abutment no. 1
610-035	Svijany	1924	in-leak, corrosion, cracks in f.f.	f.f. arc over abutment no. 1

Two sets of petrographic thin section have been prepared. First one was employed for the optical microscopy and image analysis consisted of thin sections of 50 × 50 mm. Second set (thin sections with dimensions 35 × 28 mm) was designed for the analytical study by SEM/EDS.

3 MICROSCOPIC TECHNIQUES APPLIED FOR STUDIED CONCRETES

3.1 Conventional optical microscopy

The conventional optical microscopy is one of the basic petrographic techniques during which the samples – thin sections are examined in transmitted light mode (non-polarised and polarised light). This standard technique allows identification of present mineral phases, nature of rock fragments in concrete but also cement paste or voids.

In this study, a LEICA DMLP (Optical Laboratory of the Institute of Geochemistry, Mineralogy and Mineral Resources) polarising microscope was employed. The optical microscopy served for basic description of thin sections including identification of fragment type (petrography of coarse- and fine-grained aggregates), relationship between aggregate and cement paste, type and location of voids and features related to the presence of alkali-silica gels. Moreover, the series of microphotographs were taken that later served for the petrographic image analysis.

3.2 Quantification of phases by means of petrographic image analysis

Petrographic image analysis is a technique allowing quantification of certain aspects of rock composition (e.g. volume of rock-forming minerals, volume of voids) or rock fabric (e.g. grain size, grain shape, shape of voids) on microscopic (thin sections) or macroscopic (polished hand specimens or larger) scales. Several approaches were suggested during last decades that consist either in automatic recognition of phases by software itself (e.g. Ehrlich et al. 1991, Wang 1995) or by image pre-processing by operator (petrographer) (e.g. Siegesmund et al. 1994, Přik-

ryl 2001, 2006). Because of specific optical features of rocks and similar materials, the second approach is widely recommended.
The system of petrographic image analysis employed in this study (Fig. 2), consists of the manual image pre-processing, computer image analysis and data evaluation.

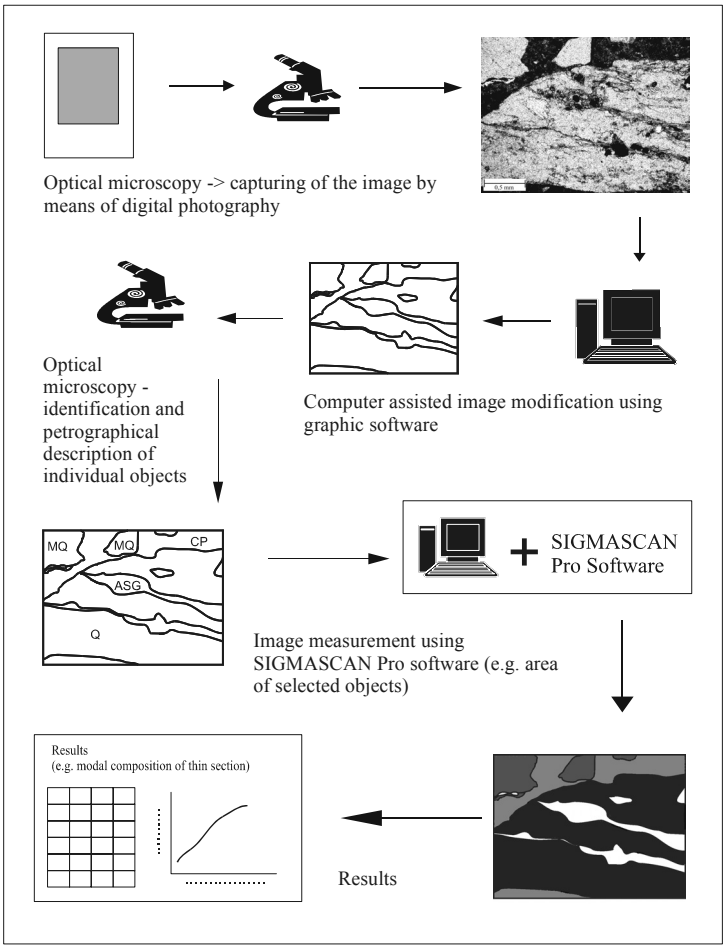

Figure 2 : Image processing of thin sections.

Image pre-processing involves capturing of the image by means of conventional or digital photography in the optical microscope, identification of measured objects, i.e. petrographic type of fragments, and image modification using graphic software (Corel Draw v. 12.0). The image modification is a crucial point in the image pre-processing because the software used (SIGMASCAN Pro by Jandel Scientific) requires binary image on which the object is detected from the background based on the intensity of greyscale. This means that the object can be made either "lighter" or "darker" than the background. In the preparatory stage, it is also important to add identifier to each of the objects that indicates its petrographic nature. This identification is necessary for multiphase materials as were the studied concrete samples. The analysis of multiphase materials requires measurement of appropriate amount of objects that ranges from 300 to 500 per sample.

Using SIGMASCAN Pro software, the image measurement is performed by feature-specific approach (i.e. fill measurement). In practice, the objects are measured separately. After the measurement each object is filled with a contrast colour to avoid multiple analyses once meas-

ured grain. Finally, the data obtained are analysed using any statistical software. More details on the image preparation and image analysis can be found elsewhere (Přikryl 2001, 2006).

3.3 SEM/EDS analysis

Scanning electron microscopy with energy diffraction analysis (SEM/EDS analysis) was conducted at the Laboratory of Electron Microscopy and Microanalysis (Laboratories of Geological Institutes, Faculty of Science, Charles University in Prague, operator R. Procházka). The measurement was carried out at Cambridge Cam Scan S4 with energy dispersive analytical system (Oxford Instruments LINK ISIS 300) under following conditions: beam current 3 nA, accelerating voltage 20 kV. SPI Suplies 53 Minerals Standard set #02753-AB was used for routine quantitative calibration. The SEM/EDS analysis facilitated identification of alkali-silica gels and verification of mineralogical composition of individual fragments previously classified by optical microscopy.

4 RESULTS

All studied samples contained coarse-grained and fine-grained aggregate, cement paste, voids and alkali-silica gels in different proportions (Tab. 2). The coarse-grained aggregate (particles larger than 4 mm) is built of angular fragments petrographically belonging to rocks differing genetically and compositionally. In general, all genetic groups of rocks were encountered. The magmatic rocks are represented by diabases and basalts.

Table 2 : Proportion of major components of studied samples as determined by petrographic image analysis. All data are in vol. %, n.d. means not determined.

	14-070	14-071	180-010	232-007	272-006	610-018	610-019	610-035
coarse-grained aggregate	26.7	30.8	36.4	22.8	42.1	51.1	38.0	40.3
fine-grained aggregate	24.9	14.8	22.4	26.3	16.0	13.6	13.5	16.1
cement paste	47.0	52.3	37.9	45.4	40.0	32.7	44.6	42.0
voids	1.3	2.0	2.6	4.9	1.3	2.3	3.2	0.8
alkali-silica gels	0.1	0.1	0.7	0.6	0.6	0.3	0.7	0.8

Table 3 : Composition of coarse-grained fraction as determined by petrographic image analysis. All data are in vol. %, n.d. means not determined.

	14-070	14-071	180-010	232-007	272-006	610-018	610-019	610-035
diabase	25.5	20.3	n.d.	n.d.	n.d.	4.0	n.d.	n.d.
basalt	1.2	6.9	4.6	n.d.	3.2	18.8	0.5	n.d.
quartzite	n.d.	n.d.	25.7	18.6	12.9	2.6	29.9	31.5
pelite	n.d.	n.d.	3.9	4.0	n.d.	n.d.	8.0	6.9
greywacke	n.d.	n.d.	n.d.	n.d.	26.1	25.9	n.d.	n.d.
carbonate	n.d.	3.4	n.d.	n.d.	n.d.	n.d.	n.d.	n.d.
slag	n.d.	n.d.	2.1	n.d.	n.d.	n.d.	n.d.	1.5

Quartzite and metapelite rock fragments are of metamorphic origin. Particles representing rocks of sedimentary origin belong to greywackes and carbonates. The studied rocks show relatively broad span both in the type of the coarse-grained particles (Tab. 3) and also in their proportion in respect to other phases.

Fine-grained aggregate (particles below 4 mm) consists of prevailing monomineral quartz that forms 80-95 % of the fine-grained fraction. The remaining amount is due to the presence of feldspars, rock fragments (granitoids, metasediments) and of artificial aggregate – slag. Except the slag particles, the fine-grained aggregates are mostly sub-rounded or rounded. There is low compositional variation in the type of fine-grained aggregate.

The amount of cement paste varies from 22.8 to 51.1 vol. % and is characterised by presence of common voids that make 0.8 to 4.9 vol. %. The alkali-silica gels were identified in all studied samples and their amount range from 0.1 to 0.8 %.

5 INTERPRETATION OF ALKALI-SILICA GELS

During inspection in 1990 and 2005 the following damages on bridges constructions were identified: in-leak into construction joints, cracks thorough spandrel panels, out-off-drainage in landing fronts and systems of cracks through face-sides and their spalling. All these failures enabled water inflow to concrete. Rarely, the presence of alkali-silica gels was manifested by white coatings on a surface of concrete.

Optical microscopy and the SEM/EDS analysis were used to verify the origin of alkali-silica gels in microscale. The gels tend to form reaction rims on the contact between cement paste and quartzite and/or greywacke rock fragments (Fig. 3). Similar "corrosion" boundaries were observed in mortar bar test specimens (Pertold et al. 2007) tested according ASTM C1260. In some cases, the gels protrude into the rock fragments. Monomineral quartz particles are rarely disturbed by ASR cracks (Fig. 3). For other types of coarse- and fine-grained particles (especially for diabase and basaltic rock fragments) no evidence exists for the occurrence of the alkali-silica gels.

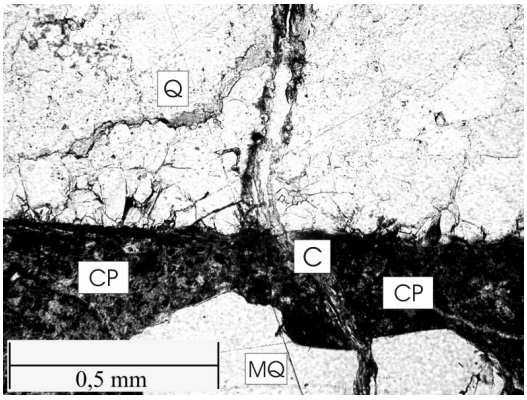

Figure 3 : Alkali-silica gel partly inlaying crack thorough quartzite and monomineral quartz fragment (Q – quartzite rock fragment, MQ - monomineral quartz fragment, CP – cement paste, C – crack partly filled by alkali-silica gel, conventional optical microscope).

The reactivity of fragments containing strained quartz is influenced by grain-size and degree of quartz deformation (e.g. Zhang et al. 1999, del Amo and Pérez 2001, Marfil and Maiza 2001, Monteiro et al. 2001, Rivard et al. 2002). Both factors can be found in studied concrete samples where quartzite fragments make dominant phase. The size of individual quartz grains in quartzite particles is less than 0.1 mm and most of the grains exhibit strong undulatory extinction. In several quartz grains, formation of subgrains and consequently their transformation to microcrystalline quartz (with diameter of grains in the range of few micrometers) was observed.

When treating the alkali-silica gels data statistically, a satisfactory correlation has been found mainly for quartzite fragments and amount of alkali silica gels (Fig. 4). The correlation factor (R^2) makes 0.895. The similar correlation factor (R^2 = 0.827) was obtained when comparing amount of alkali-silica gels and year of the bridges' construction (Fig. 4).

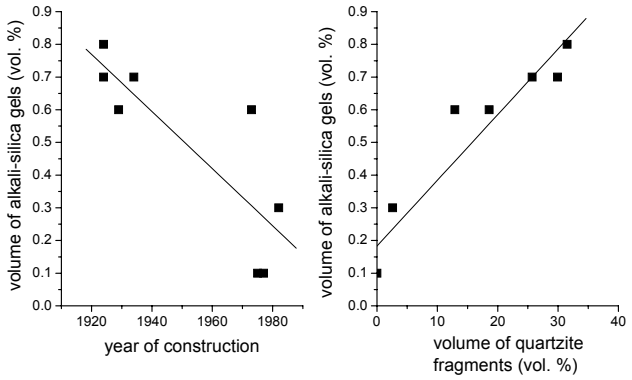

Figure 4 : (left part) Correlation between volume of alkali-silica gels and amount of quartzite fragments. (right part) Correlation between volume of alkali-silica gels and period of bridge construction.

Time is another factor affecting the ASR development (Grattan-Bellew 1997, RILEM AAR-0). The studied bridges can be subdivided into two groups based on the period of their construction: First group is represented by those built in 1920-1930s, the other group in 1970-1980s. Concrete samples taken from the first group show generally higher volumes of the alkali-silica gels than the second group (Fig. 3). The younger group is, however, less homogeneous when considering amount of alkali-silica gels. One bridge constructed in 1973 shows the same level of alkali-silica gels as the first group (compare Figure 4), which is probably caused by higher proportion of quartzite and greywacke rock fragments (compare Table 3) than in other concrete samples taken from the younger group of bridges. Another bridge, constructed in 1982, shows also higher amount of gels, probably not only due to high proportion of greywacke fragments but also due to the presence of diabase and basalt particles that are also considered to be potentially reactive. Remaining two younger bridges are free of reactive rock fragments and thus show very low amount of alkali-silica gels. This observation supports idea that the ASR is primarily controlled by the presence of reactive particles and their amount.

6 CONCLUSIONS

Based on detailed petrographic analysis (optical microscopy of thin sections, quantitative petrographic image analysis, SEM/EDS analysis) it has been possible to determine percentage of present components of studied concrete samples, to locate the alkali-silica gels and to determine their relationship to the certain type of aggregate. Regarding the methodology, the petrographic image analysis is the only technique allowing quantification of the data obtained during optical microscopy. The conventional optical microscopy is, however, necessary for the identification of present phases.

Based on the combination of the optical microscopy and petrographic image analysis, the studied concrete samples consist of coarse- and fine-grained aggregates, cement paste, voids and alkali-silica gels. The major compositional and volumetric variations have been found for the coarse-grained aggregate.

The presence of alkali-silica gels, previously inferred from cracks and failures on bridges constructions, is clearly microscopically manifested by microcracks disturbing the rock fragments and forming reaction rims on the contact between aggregate fragments and cement paste. Presence of two genetically different types of coarse-grained aggregates – quartzite and greywacke has been found as the critical factor controlling ASR. These two components show, however, similarity in presence of reactive or possibly reactive forms of SiO_2 (strained quartz in quartzite or poorly crystalline silica in greywacke). Just subtle signs of ASR were located for

monomineral quartz fragments. Other coarse- and fine-grained particles show no evidence of alkali-silica gels.

The time-dependence of alkali-silica gels formation is obvious from comparison of bridges constructed in 1920-1930s with those constructed in 1970-1980s. The amount of alkali-silica gels can be higher in younger structures if larger proportion of reactive components is present.

ACKNOWLEDGEMENT

This study was undertaken as a part of the project no. 1F45C/096/120 supported by the Ministry of Transport of the Czech Republic. The finance from the project MSM0021620855 "Material flow mechanisms in the upper spheres of the Earth" is acknowledged as well.

REFERENCES

del Amo, D.G. and Pérez, B.C. 2001. Diagnosis of the alkali-silica reactivity potential by means of digital image analysis of aggregate thin sections. *Cement and Concrete Research* 31, p. 1449-1454.

ČSN 736221. 1996. Revision of bridge roads.

Ehrlich, R., Crabtree, S.J., Horkowitz, K.O. and Horkowitz, J.P. 1991. Petrography and Reservoir Physics: I, II and III. *American Association of Petroleum Geologists Bulletin* 75, p. 1547-1562.

Hobbs, D.W. 1988. *Alkali-silica reaction in concrete*. London: Thomas Telford.

Grattan-Bellew, P.E. 1997. A Critical Review of Ultra-accelerated Tests for Alkali-silica Reactivity. *Cement and Concrete Composites* 19, p. 403-414.

Klier T., 2006. MPM. Technical Report.

Koskiahde, A. 2004. An experimental petrographical classification scheme for the condition assessment of concrete in façade panels and balconies. *Materials Characterisation* 53(2-4), p. 327-334.

Marfil, S.A. and Maiza, P.J. 2001. Deteriorated pavements due to the alkali-silica reaction. A petrographic study of three cases in Argentina. *Cement and Concrete Research* 31(7), p. 1017-1021.

Monteiro, J.M.P., Shomglin, K., Wenk, R.H. and Hasparyk, N.P. 2001. Effect of Aggregate Deformation on Alkali-Silica Reaction. *ACI Materials Journal* 98(2), p. 179-183.

Pertold, Z., Lukschová Š., Přikryl R. 2007. *Identification of alkali-silica reactivity of aggregate in concrete and its causes*. Unpublished technical report, Charles University in Prague, p. 72. (In Czech)

Peterson, K., Gress, D., Van Dam, T. and Sutter, L. 2006. Crystallised alkali-silica gel in concrete from the late 1890s. *Cement and Concrete Research* 36(8), p. 1523-1532.

Přikryl, R. 2001. Some microstructural aspects of strength variation in rocks. *International Journal of Rock Mechanics and Mining Sciences & Geomechanical Abstracts* 38(5), p. 671-682.

Přikryl, R. 2006. Assessment of rock geomechanical quality by quantitative rock fabric coefficients: Limitations and possible source of misinterpretations. *Engineering Geology* 87(3-4), p. 149-162.

RILEM-AAR 0. 2002. Outline Guide to the Use of RILEM Methods in Assessments of Aggregates for Potential Alkali-Reactivity. RILEM Technical Committee TC ARP.

Rivard, P. and Ballivy G. 2005. Assessment of the expansion related to alkali-silica reaction by the Damage Rating Index method. *Construction and Building Mterials* 19(2), p.83-90.

Rivard, P., Ollivier, J-P. and Ballivy, G. 2002. Characterization of the ASR rim. Application to the Potsdam sandstone. *Cement and Concrete Research* 32(8), p. 1259-1267.

Rivard, P., Fournier, B. and Ballivy, G. 2000. Quantitative petrographic technique for concrete damage due to ASR: Experimental and application. *Cement Concrete and Aggregates* 22(1), p.63-72.

Sahu, S. and Thaulow, N. 2004. Delayed ettringite formation in Swedish concrete railroads ties. *Cement and Concrete Research* 34(9), p. 1675-1681.

Siegesmund, S., Helming, K. and Kruse, R. 1994. Complete texture analysis of a deformed amphibolite – comparison between neutron diffraction and U-stage data. *Journal of Structural Geology* 16(1), p. 131-142.

St John, D.A., Poole, A.B. and Sims, I. 1998. *Concrete petrography. A handbook of investigative techniques*. London: Arnold.

Wang, L. 1995. Automatic identification of rocks in thin sections using texture analysis. *Mathematical Geology* 27(7), p. 847-865.

Zhang, C., Wang, A., Tang, M. Wu, B. and Zhang, N. 1999. Influence of aggregate size and aggregate size grading on ASR expansion. *Cement and Concrete Research* 29, p. 1393-1396.